2009-03-06

Near-Optimal Antenna Design for Multiple Antenna Systems

Daniel N. Evans
Brigham Young University - Provo

NEAR-OPTIMAL ANTENNA DESIGN FOR

MULTIPLE ANTENNA SYSTEMS

by

Daniel N. Evans

A thesis submitted to the faculty of

Brigham Young University

in partial fulfillment of the requirements for the degree of

Master of Science

Department of Electrical and Computer Engineering

Brigham Young University

April 2009

BRIGHAM YOUNG UNIVERSITY

GRADUATE COMMITTEE APPROVAL

of a thesis submitted by

Daniel N. Evans

This thesis has been read by each member of the following graduate committee and by majority vote has been found to be satisfactory.

Date	Michael A. Jensen, Chair

Date	Karl F. Warnick

Date	Brain D. Jeffs

BRIGHAM YOUNG UNIVERSITY

As chair of the candidate's graduate committee, I have read the thesis of Daniel N. Evans in its final form and have found that (1) its format, citations, and bibliographical style are consistent and acceptable and fulfill university and department style requirements; (2) its illustrative materials including figures, tables, and charts are in place; and (3) the final manuscript is satisfactory to the graduate committee and is ready for submission to the university library.

_____   _____
Date   Michael A. Jensen
                                                       Chair, Graduate Committee

Accepted for the Department

                                                       _____
                                                       Michael J. Wirthlin
                                                       Graduate Coordinator

Accepted for the College

                                                       _____
                                                       Alan R. Parkinson
                                                       Dean, Ira A. Fulton College of
                                                       Engineering and Technology

ABSTRACT

NEAR-OPTIMAL ANTENNA DESIGN FOR

MULTIPLE ANTENNA SYSTEMS

Daniel N. Evans

Department of Electrical and Computer Engineering

Master of Science

Multiple-input-multiple-output (MIMO) wireless systems use multiple antenna elements at the transmitter and receiver to offer improved spectral efficiency over traditional single antenna systems. In these systems, properties of the transmit and receive antenna arrays play a key role in determining the overall performance of the system. This thesis derives an upper bound on ergodic (average) channel capacity which formally links good antenna diversity performance with good ergodic capacity. As a result of this derivation, antenna arrays with good ergodic capacity performance are designed in this thesis by designing antenna arrays with near-optimal diversity gain.

Several approaches are developed to design antenna array elements which achieve near-optimal diversity. These design methods only require an array geometry and the power azimuth spectrum of the propagation environment. Examples and analysis are included that illustrate advantages and disadvantages of each design technique. Three different array geometries are also investigated. Diversity

performance results for each design technique and array geometry, averaged over an ensemble of typical power azimuth spectrums, are presented and compared. This analysis shows that the diversity gain achieved by the best design approach is, on average, less than 1.5 dB below the optimal diversity gain.

ACKNOWLEDGEMENTS

Table of Contents

List of Tables

List of Figures

Chapter 1

Introduction

The use of wireless local area networks is continually increasing in our complex world. One key challenge associated with these networks is that they are typically employed in environments characterized by multipath radiowave propagation, making reliable and high-rate communications very difficult. In addition, network users demand ever-increasing throughput at a time when frequency spectrum is scarce.

One approach for improving the communication reliability and throughput of networks operating in multipath environments is to employ multiple antennas, referred to as multiple-input-multiple-output (MIMO) technology, to increase spectrum efficiency. A large volume of research has appeared on this topic, and in fact the technology has matured to the point that it is being implemented in emerging wireless systems. Multiple antenna systems are especially interesting because of the dramatic potential improvement they offer in capacity [1]. The successful implementation of a MIMO system that achieves significant capacity gains over conventional wireless systems depends on a number of key elements. One key element to the overall performance of any MIMO system is the design of the antenna arrays at each end of the link.

Experimental results presented in [2] verify that the design of the antenna arrays at each end of the link dramatically influences the channel capacity. Recent work has formulated the *Intrinsic Capacity* for a specific channel independent of the transmit and receive antenna characteristics [3]. This provides an upper bound which aids in identifying antenna elements and arrays that provide near-optimal capacity, but does not provide a synthesis approach. Although the community

is currently very adept at predicting the performance of a MIMO system given a specific antenna arrangement and multipath channel [1], the question of how to synthesize antennas that approach the optimal performance bound remains an open topic of research [4].

Studies have demonstrated some general criteria regarding the antenna radiation patterns that deliver good performance in typical environments. For example, the work in [5] shows that performance is improved when antennas direct power where most of the multipath components are concentrated, usually the horizontal plane. In addition, it has become common practice among antenna designers to seek antenna arrays whose element radiation patterns are orthogonal [6]. However, this rule-of-thumb is only ideal when multipath is equally likely to arrive from all angles. Using another approach to address this question, research has shown that an intelligently-selected sub-array can improve performance in relation to the performance of a fixed array [7,8]. This previous research is valuable; nonetheless an effective and practical approach for antenna synthesis that relies only on average propagation behavior at one end of the link has yet to be developed.

In [9] a physically impractical synthesis approach is presented that finds antenna radiation patterns that optimize diversity, given stochastic characteristics of the propagation environment at one end of the link and an aperture within which each antenna must reside. This thesis builds directly onto that work. The results in [9] are very interesting but would be more significant if there existed a derivation relating optimal diversity performance to near-optimal capacity. Also a physically practical synthesis approach must be devised as opposed to the optimal but physically impossible approach described in [9].

1.1 Thesis Contributions

This thesis directly addresses the issue of creating an effective and practical approach for the synthesis of near-optimal MIMO antenna arrays based only on average propagation behavior at one end of the link. Specifically, the contributions of this thesis are:

1. The derivation of an upper bound on ergodic capacity that links good diversity performance with good ergodic capacity. This upper bound on ergodic capacity is verified through numeric simulation.

2. The development and comparison of several different practical design approaches to approximate the antenna radiation patterns that optimize diversity performance. This includes a discussion of the advantages and disadvantages of each of the design approaches developed.

3. The analysis of three unique and practical antenna array geometries and their performance in multipath environments.

4. A study quantifying the performance benefits of the elaborate design techniques described in this thesis over very simple dipole antenna arrays. This study also addresses how the difference in performance of these two types of arrays is affected by the richness of the multipath.

1.2 Thesis Organization

The remainder of this thesis is organized as follows. In Chapter 2, background information essential to the understanding of the research contained in this thesis is introduced. This includes discussions on the modeling of multipath, effects of channel correlation, and a single-valued performance metric of antenna diversity. Chapter 2 also includes a section that reviews some of the work from [9] since that work is foundational to this thesis. A derivation linking diversity and capacity performance and sample data showing ergodic capacity as a function of diversity is in Chapter 3.

Chapter 4 develops several different antenna design methods that achieve near-optimal diversity performance. In Chapter 5 average results are calculated for each of the design methods developed. Several examples are presented to investigate the advantages and disadvantages of each design approach. Some experiments that address the influence of array geometry on performance are also included. Chapter 6 clearly states conclusions drawn from the previous chapters.

In addition, it explains the contributions of this work and the recommendations for future related research.

Chapter 2

Background Research

There has been extensive research and excitement about the idea of using multiple antennas at each end of a wireless communication link to obtain data rates much higher than what is possible using traditional single antenna systems. The fundamental idea of these multiple antenna communication systems is to take advantage of the complexity of multipath propagation environments typical of urban and indoor scenarios. This chapter briefly discusses the basic MIMO model along with other important topics such as channel correlation, multipath modeling, and previous research focused on optimal antenna design for multiple antenna systems.

2.1 MIMO Model

In a typical MIMO system there are N transmit antennas and M receive antennas. Let the N x 1 vector $\mathbf{x}$ contain N complex baseband symbols, each of which is transmitted by one of the N transmit antennas. Furthermore, let the complex baseband transfer function between the nth transmit and m^{th} receive antenna be denoted as H_{mn}. If each element of the M x 1 vector $\mathbf{y}$ represents the complex baseband signal received by each receive antenna, we can write

$$\mathbf{y} = \mathbf{H}\mathbf{x} + \boldsymbol{\eta}, \tag{2.1}$$

where H_{mn} represents the mn^{th} element of the M x N matrix $\mathbf{H}$ and $\boldsymbol{\eta}$ is an M x 1 vector of noise consisting of zero-mean independent Gaussian random variables with variance σ_η^2. Under these circumstances, if $\mathbf{H}$ is known and nonsingular, the

maximum-likelihood estimate of $\mathbf{x}$ can be computed at the receiver by the operation $\hat{\mathbf{x}} = \mathbf{H}^{-1}\mathbf{y}$.

Given that the transmitter has channel state information (CSI), transmit power can be allocated so as to maximize the capacity of the channel [10]. Transmitter power allocation is characterized by the transmit covariance matrix, defined as

$$\mathbf{Q} = \mathrm{E}\left[\mathbf{x}\mathbf{x}^{\dagger}\right], \tag{2.2}$$

where E[·] indicates expectation and $(\cdot)^{\dagger}$ denotes conjugate transpose. The total transmit power is given by

$$P_T = \mathrm{tr}(\mathbf{Q}), \tag{2.3}$$

where tr(·) indicates summing the diagonal elements of the matrix (trace). The water-filling solution [11] is a well known technique to find the $\mathbf{Q}$ that maximizes the channel capacity given the maximum transmit power constraint of P_T. Details of the water-filling solution are presented in Section 3.2.

2.2   Channel Correlation

Small changes in the location of either the transmitter or receiver, or small perturbations to the channel can dramatically change the channel matrix [12]. These fluctuations in $\mathbf{H}$ create problems when attempting to design a multiple antenna system that works well over an ensemble of channel matrices. However, it has been shown in [13] that the channel correlation, defined as

$$\mathbf{R}_H = \mathrm{E}\left[\mathrm{vec}(\mathbf{H})\,\mathrm{vec}(\mathbf{H})^{\dagger}\right], \tag{2.4}$$

where vec(·) indicates columnwise stacking of the matrix into a *MN* x 1 vector, remains relatively constant over reasonable distances (quasi-stationary process). Because of this, with knowledge of the channel correlation the transmitter is able to direct energy to produce good *average* signal-to-noise ratio (SNR) at the receiver,

6

without requiring frequent and costly updates of the channel matrix at the transmitter.

Under the assumption that the correlation at the receiver is independent of that at the transmitter, the channel correlation can be written in the simpler form

$$\mathbf{R}_H = \mathbf{R}_R \otimes \mathbf{R}_T, \qquad (2.5)$$

where $\mathbf{R}_R = \mathrm{E}\left[\mathbf{H}\mathbf{H}^\dagger\right]$ and $\mathbf{R}_T = \mathrm{E}\left[\mathbf{H}^\dagger\mathbf{H}\right]$ are referred to as the receive and transmit correlation matrices respectively and $\otimes$ indicates the Kronecker product [14]. The Kronecker product approximation is experimentally validated in [15]. This approximation is important because equation (2.5) suggests characterizing the channel correlation matrix by the correlation at each end of the channel. Since the goal of this work is the design of antennas for multi-antenna systems and since the correlation depends on the antenna arrays as well as the propagation environment, this separation is critical because it allows independent design of the antennas at the transmitter and receiver.

2.3 Diversity Gain

The signal received by an antenna can vary widely in phase and magnitude as a result of the propagation environment. The result of these variations in received signal is that the wireless link will at times fade, resulting in a receive SNR too low to recover the transmitted signal. Perhaps the most straightforward way to reduce the likelihood of a deep signal fade is to have multiple receive antennas, each with a unique position or pattern, and combine the signals received in a constructive way. This antenna diversity method works simply because it is not likely that all receive antennas will fade simultaneously. To achieve optimal performance, the received signals should be combined using a method known as maximal ratio combining [16] in which each received signal is shifted to a common phase and then weighted such that the sum of the signals maximizes the SNR. The results in this thesis assume the use of maximal ratio combining.

The performance of antenna diversity systems is typically defined probabilistically. Consider a diversity system with M antennas, where the signals on the branches are uncorrelated and each has an average SNR of Γ. The probability that the SNR of the output of a maximal ratio combiner, denoted as γ, is less than some threshold x is given by

$$P(\gamma \leq x) = 1 - e^{-x/\Gamma} \sum_{k=1}^{N_r} \frac{(x/\Gamma)^{k-1}}{(k-1)!}. \tag{2.6}$$

Figure 2.1 plots this cumulative distribution function (CDF) for normalized SNR and different numbers of antennas. As can be seen, as more antennas are used, the probability of a deep fade reduces dramatically.

With this performance description in mind we can define a single-valued performance metric, referred to as the diversity gain. To do so, we first set a probability threshold. For example, acceptable operation of our system requires that the SNR remain above a certain level 99% of the time, we let our threshold be $1 - .99 = .01$ (this is the threshold used throughout this thesis). For one antenna, Figure 2.1 reveals that the normalized SNR is above -20 dB 99% of the time. For two antennas, the normalized SNR is higher than -9 dB 99% of the time. The addition of the second antenna therefore produces a diversity gain of roughly 11 dB at the probability threshold of 1% (.01). Table 2.1 gives more precise numbers for the diversity gain as a function of the number of antennas at this 1% probability threshold. It is important to note that this example assumes that each additional branch is completely uncorrelated with the previous branches.

Table 2.1: Diversity Gain vs. Number of Uncorrelated Antennas
at 1% Probability Threshold

Number of Uncorrelated Signals Received	2	3	4	5	6
Diversity Gain in dB (relative to one signal)	11.7	16.4	19.1	21.0	22.6
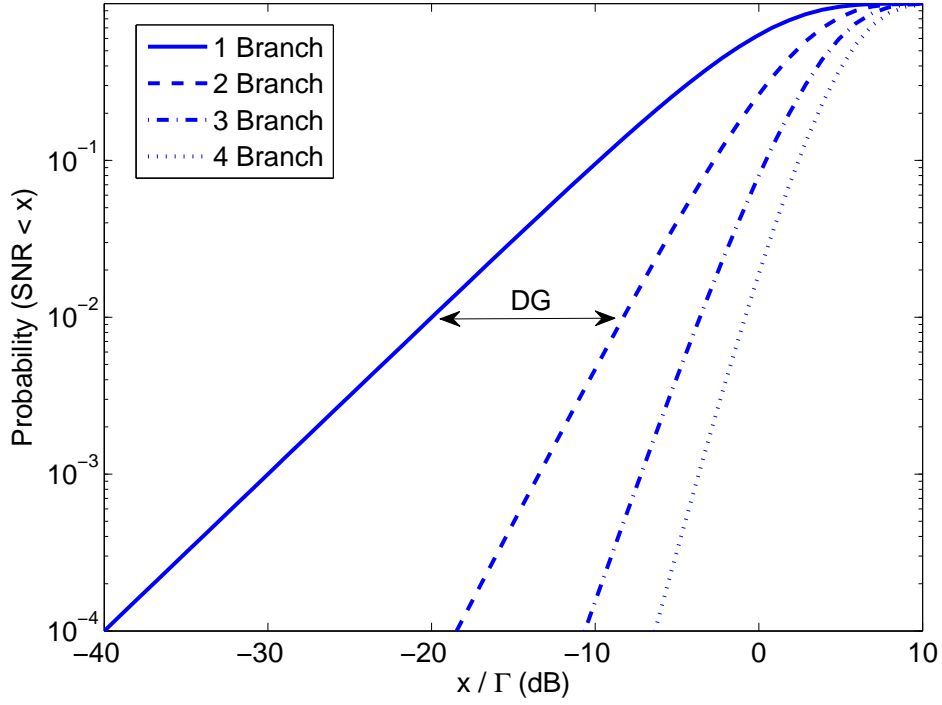
Figure 2.1: CDF of the normalized SNR for different numbers of antennas for maximal ratio combining.

In a multiple antenna system with correlated antennas, the channel correlation matrix is the quantity needed to determine the diversity gain performance. In [17] it is shown that for systems with correlated, unequal SNR branches, diversity gain can be computed by creating an equivalent system of uncorrelated antennas with branch gains equal to the eigenvalues of the correlation matrix. This implies that the channel correlation matrix which optimizes diversity gain should have large diagonal elements and off diagonal elements equal to zero.

2.4   Multipath Model

When considering the design of transmit and receive antennas it is beneficial to know the angles of departure and arrival of the signals at the transmitter and receiver, respectively. In typical complex propagation environments, the power arriving at a receiver varies widely in magnitude as a function of angle. In this

thesis, this variation in power over angle is modeled using the power azimuth spectrum (PAS) concept presented in [18]. In order to simplify modeling, the PAS is only defined for azimuth angles, meaning that propagation is confined to the horizontal plane. Figure 2.2 shows an example of a typical PAS.
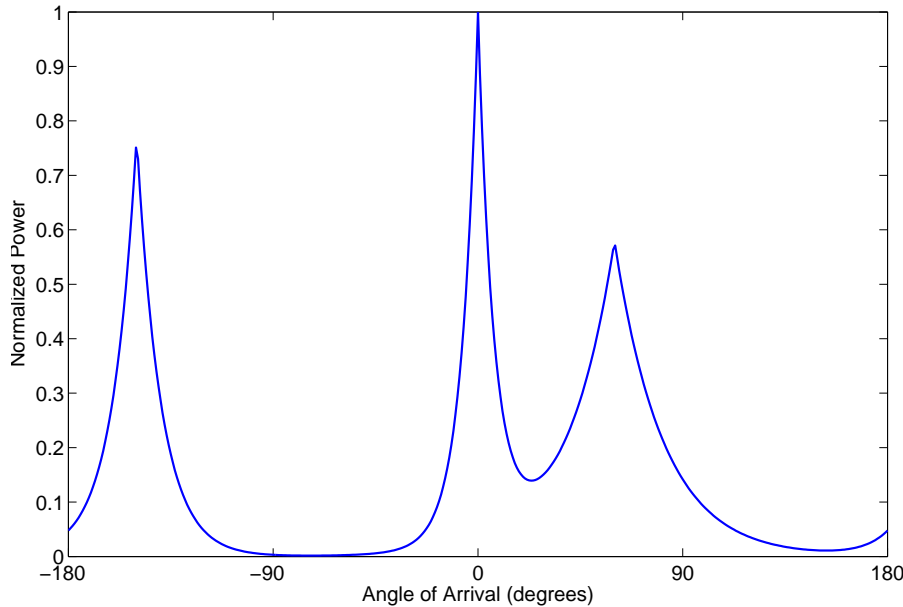
Figure 2.2: Typical power angular spectrum used to model arriving signals.

As explained in [18], the PAS of a single cluster of multipaths is commonly described by a truncated Gaussian, truncated Laplacian, or uniform distribution function. It is shown in [19] that often, especially in urban environments, a PAS has multiple such clusters centered at different angles. This PAS model is used throughout this thesis in the design of optimal antennas. It is important to remember that although the PAS model may be more intuitive on the receive end of the channel, it can be applied to the transmitter as well.

10

2.5 Summary of Previous Optimal Antenna Array Design Research

The research presented in this thesis is founded on parts of the research presented in [9]. Specifically, this thesis relies on the optimal antenna array derivation in [9]. In the presence of a known PAS, this derivation solves for multiple unique current distributions over a given aperture, each of which is referred to as an antenna. This derivation is constructed so that the antennas it produces achieve the optimal diversity gain.

Throughout this thesis the solutions to this derivation are called current distributions, which implies that transmit antennas are being designed. It is important to realize that this design approach can be used for transmit and receive antennas. For receive antennas, the results of this approach could be called weighting distributions as they represent weights applied to the received field across the receiving aperture.

The solutions to this derivation are impractical to physically implement because multiple unique current distributions cannot exist at the same time and space. However, it does provide an upper bound for diversity gain performance and a solid foundation for the ideas presented later in this thesis.

2.5.1 Summary of Optimal Antenna Array Derivation

This section is meant to give a background summary of the general design approach described in [9]. In this derivation and throughout this entire thesis all of the electric fields have $\hat{z}$ polarization. Consequently, the vector field notation is suppressed by expressing vector field quantities as scalar fields. The complete vector field formulation and more extensive explanations of this derivation are found in [9].

1. The key quantity in this derivation is the correlation matrix. In [9, 20] it is shown that the mn^{th} element of the correlation matrix is

$$R_{mn} = \varphi \int e_m(\phi)p(\phi)e_n^*(\phi)d\phi, \qquad (2.7)$$

where $e_m(\phi)$ is the electric field radiation pattern of the mth antenna, $p(\phi)$ is the power azimuth spectrum, φ is a constant, and $(\cdot)^*$ signifies complex conjugate. The constant φ is not important for this derivation and is omitted from the remaining steps.

2. Define a 2-D aperture over which any current distribution can reside. (Since the PAS model is only defined in the xy plane, the 2-D aperture can be thought of as the cross-section of an infinite cylinder perpendicular to that plane.)

3. Sample the current distribution with an orthonormal set of basis functions. In this thesis, this set is chosen to be a grid covering the aperture of equally spaced $\hat{z}$ directed pulse basis functions. If $J_m(\mathbf{r})$ represents the current distribution for the mth antenna, this expansion can be written as

$$J_m(\mathbf{r}) = \sum_n B_{nm} f_n(\mathbf{r}), \tag{2.8}$$

where f_n is the nth basis function and B_{nm} is the unknown weighting coefficient of the nth basis function in the mth current distribution.

4. Calculate the far field radiation pattern for each of the basis functions. The radiated field from the nth basis function is given as

$$z_n(\phi) = \int_V g(\phi, \mathbf{r}) f_n(\mathbf{r}) d\mathbf{r}, \tag{2.9}$$

where $g(\phi, \mathbf{r})$ is the scalar Green's function relating the currents to the far-field radiation. The radiation pattern of the mth current distribution is given by [21]

$$e_m(\phi) = \int_V g(\phi, \mathbf{r}) J_m(\mathbf{r}) d\mathbf{r} = \sum_n B_{nm} z_n(\phi). \tag{2.10}$$

5. To maximize diversity gain, as explained in Section 2.3, current distributions must be found that maximize the diagonal elements of the correlation matrix and minimize its off diagonal elements. By substituting equation (2.10) into

equation (2.7) we obtain

$$\mathbf{R} = \mathbf{B}^T \mathbf{C} \mathbf{B}^*, \tag{2.11}$$

where $(\cdot)^T$ indicates transpose, the mth column of $\mathbf{B}$ represents the mth current distribution and the matrix $\mathbf{C}$ is defined as

$$C_{nm} = \int z_m(\phi) p(\phi) z_n^*(\phi) d\phi. \tag{2.12}$$

To solve for $\mathbf{B}$, two constraints must first be placed on the solution. First, in order to have a meaningful result, all of the radiation patterns must be normalized so that they have the same radiated power. Second, if each basis function is considered lossless, impractical supergain solutions arise [22]. This can be avoided by specifying a radiation efficiency for each basis function, which is mathematically introduced through a loss resistance R_L for each basis function. These constraints lead to the equations

$$\hat{\mathbf{C}} = \hat{\mathbf{A}}^{-1/2} \mathbf{C}^T \hat{\mathbf{A}}^{-1/2}, \tag{2.13}$$

$$\mathbf{b}_m^\dagger \hat{\mathbf{A}} \mathbf{b}_m = P_d, \tag{2.14}$$

$$\hat{\mathbf{A}} = \mathbf{A} + R_L \mathbf{I}, \tag{2.15}$$

$$A_{nm} = \frac{1}{2\eta_0} \int z_n^*(\phi) z_m(\phi) d\phi, \tag{2.16}$$

where $\mathbf{b}_m$ represents the mth column of $\mathbf{B}$, P_d is the power delivered to the array, R_L is the loss resistance associated with each basis function, $\mathbf{I}$ is the identity matrix, and η_0 is the characteristic impedance of free space. Finally, it has been shown in [9] that $\mathbf{R}$ is diagonal and its diagonal elements are maximized when the current distributions are chosen to be

$$\mathbf{B} = P_d^{1/2} \hat{\mathbf{A}}^{-1/2} \mathbf{\Sigma}, \tag{2.17}$$

where $\mathbf{\Sigma}$ is a unitary matrix of the eigenvectors of $\hat{\mathbf{C}}$.

2.5.2   Summary of Optimal Antenna Array Results

Some results obtained using the solution method discussed previously are presented here to establish background for this thesis. For the purposes of this thesis, the radiation efficiency of the basis functions is always assumed to be 99%.

Before meaningful examples can be considered, the number of different antennas needed to create good diversity needs to be addressed. If N_b basis functions are used to sample each aperture, the solution yields N_b current distributions that when taken together produce the optimal diversity gain. If N_b is large (which is typical when trying to accurately model currents), it is impractical to build a diversity system using all N_b antennas. Fortunately, considering the current distributions corresponding to the N_e largest eigenvalues of $\hat{\mathbf{C}}$ yields optimal performance for a system with N_e antennas. In addition, the diversity gain using N_e antennas quickly approaches the diversity gain achieved using N_b antennas, even for values of N_e much less than N_b. Figure 2.3 shows how the optimal diversity gain of a λ x λ square aperture varies as a function of the number of antennas used. For the results presented here $N_b = 100$ and the PAS is a simple truncated Gaussian.

To make this example more tractable, only the solutions corresponding to the four largest eigenvalues are considered ($N_e = 4$). This example examines the current distributions and radiation patterns produced by the solution method. Consider a λ x λ square aperture, sampled by 100 equally spaced pulse functions, in the presence of the PAS in Figure 2.2. The diversity gain of the optimal array is 20.2 dB relative to a single Hertzian dipole. Throughout this thesis, unless stated otherwise, diversity gain is calculated relative to a single Hertzian dipole. The optimal radiation patterns and current distributions are shown in Figures 2.4 and 2.5, respectively. As expected, an obvious correlation between the PAS and the antenna radiation patterns can be observed.
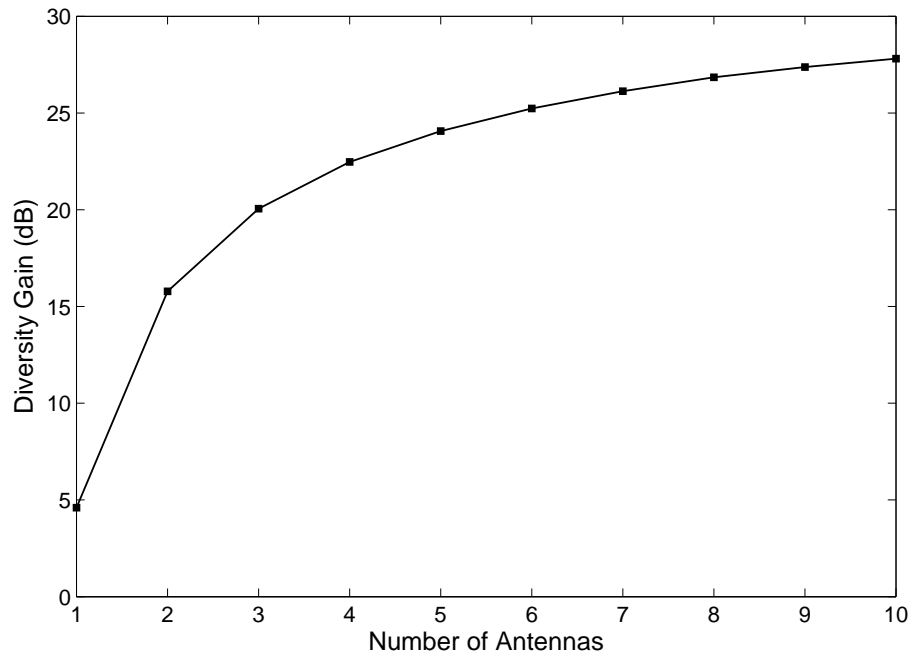
Figure 2.3: Diversity gain vs. number of antennas for a $\lambda \times \lambda$ aperture with 100 basis functions.
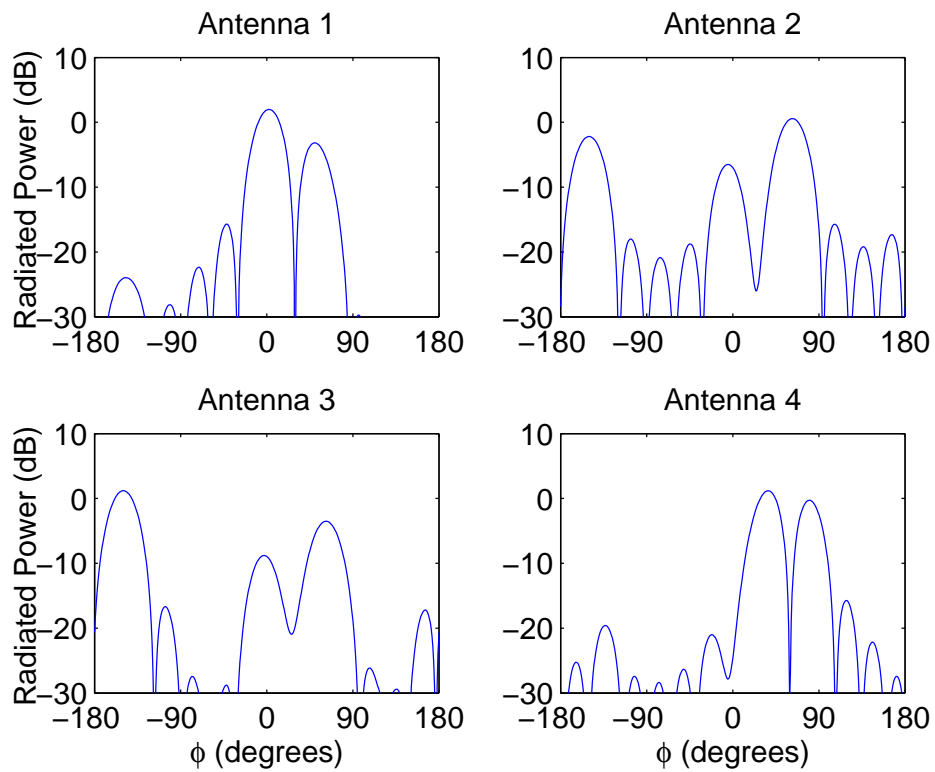
Figure 2.4: Optimal radiation patterns for a $\lambda \times \lambda$ aperture, given the PAS in Figure 2.2.
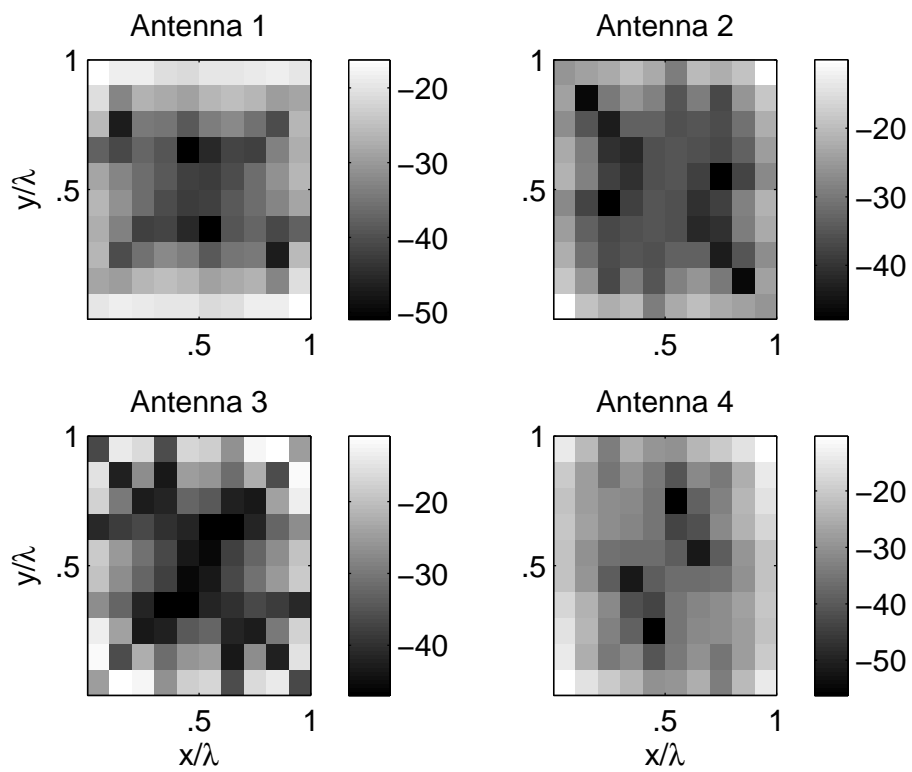
Figure 2.5: Magnitude of optimal currents over a λ x λ aperture, given the PAS in Figure 2.2.

Chapter 3

Connection between Diversity Gain and Capacity

The synthesis approach described in [9] is optimal in the sense that it maximizes the diversity gain. A fundamental assumption to the work in [9] is that maximizing the diversity gain also maximizes the capacity. Although it is intuitive to believe that maximizing the diversity gain maximizes the capacity, a proof of this relationship has yet to be completed. The purpose of this chapter is to show that maximizing diversity gain produces good ergodic capacity.

3.1 Derivation of Upper Bound for Ergodic Capacity

It is well known [1, 23] that the capacity of a MIMO link is given by

$$C = \max_{\mathbf{Q}} \log \left(\det \left(\mathbf{I}_M + \frac{\mathbf{HQH}^\dagger}{\sigma_\eta^2} \right) \right), \tag{3.1}$$

where $\mathbf{I}_M$ is the identity matrix with dimensions M x M. As defined previously, $\mathbf{H}$, $\mathbf{Q}$, and σ_η^2 represent the channel matrix, transmit covariance matrix, and noise power, respectively. The transmit covariance matrix has the constraint that $\text{tr}(\mathbf{Q}) = P_T$. The ergodic capacity of the channel is the expected value of the capacity,

$$C_e = \max_{\mathbf{Q}} \text{E} \left[\log \left(\det \left(\mathbf{I}_M + \frac{\mathbf{HQH}^\dagger}{\sigma_\eta^2} \right) \right) \right]. \tag{3.2}$$

Using the matrix identity that $\det(\mathbf{I} + \mathbf{AB}) = \det(\mathbf{I} + \mathbf{BA})$ and the fact that $\log(\det(\cdot))$ is a concave function [24, 25], one can use Jensen's inequality [26] to obtain the upper bound

$$C_e \leq C_u = \max_{\mathbf{Q}} \log \left(\det \left(\mathbf{I}_M + \frac{\text{E}[\mathbf{H}^\dagger\mathbf{H}]\mathbf{Q}}{\sigma_\eta^2} \right) \right). \tag{3.3}$$

Recalling that

$$\mathbf{R}_T = E[\mathbf{H}^\dagger \mathbf{H}], \tag{3.4}$$

we arrive at an upper bound in terms of the transmit channel correlation matrix given by

$$C_u = \max_{\mathbf{Q}} \log\left(\det\left(\mathbf{I}_M + \frac{\mathbf{R}_T \mathbf{Q}}{\sigma_\eta^2}\right)\right). \tag{3.5}$$

The upper bound (3.5) is very similar to the result obtained in [27] with the difference being that in [27], $\mathbf{Q} = \beta\mathbf{I}$ while here $\mathbf{Q}$ is allowed to be arbitrary. Physically, removing this constraint on $\mathbf{Q}$ allows power to be allocated optimally in order to increase capacity.

3.2 Solving for the Upper Bound

In order to solve for the capacity's upper bound, the value of $\mathbf{Q}$ that maximizes (3.5) must be found. This is accomplished by using the water-filling solution. We begin by performing an eigenvalue decomposition of $\mathbf{R}_T$ which yields

$$C_u = \max_{\mathbf{Q}} \log\left(\det\left(\mathbf{I}_M + \frac{\xi\Lambda\xi^\dagger\mathbf{Q}}{\sigma_\eta^2}\right)\right). \tag{3.6}$$

By letting $\tilde{\mathbf{Q}} = \xi^\dagger\mathbf{Q}\xi$ we obtain

$$C_u = \max_{\tilde{\mathbf{Q}}} \log\left(\det\left(\mathbf{I}_M + \frac{\tilde{\mathbf{Q}}\Lambda}{\sigma_\eta^2}\right)\right). \tag{3.7}$$

Since $\det(\mathbf{A}) \le \prod_i A_{ii}$,

$$C_u \le \max_{\tilde{\mathbf{Q}}} \sum_{i=1}^{T} \log\left(1 + \frac{\tilde{Q}_{ii}\lambda_i}{\sigma_\eta^2}\right), \tag{3.8}$$

where λ_i is the ii^{th} element of Λ. Equality is achieved when $\tilde{\mathbf{Q}}\Lambda$ is diagonal, which implies $\tilde{\mathbf{Q}}$ is diagonal. Since we want to maximize C_u, we restrict $\tilde{\mathbf{Q}}$ to be diagonal. The upper bound on the capacity becomes

$$C_u = \max_{\{\tilde{Q}_{ii}\}} \sum_{i=1}^{T} \log\left(1 + \frac{\tilde{Q}_{ii}\lambda_i}{\sigma_\eta^2}\right), \tag{3.9}$$

18

with the constraint that

$$\sum_{i=1}^{N} \tilde{Q}_{ii} = P_T, \qquad (3.10)$$

where P_T is the maximum transmit power. Using a Lagrange multiplier formulation [26] leads to

$$V = \sum_{i=1}^{T} \log\left(1 + \frac{\tilde{Q}_{ii}\lambda_i}{\sigma_\eta^2}\right) + \gamma\left(\sum_{i=1}^{T} \tilde{Q}_{ii} - P_T\right), \qquad (3.11)$$

which can be maximized by taking the partial derivative with respect to $\tilde{Q}_{ii}$ and setting it equal to zero. This gives

$$\frac{\partial V}{\partial \tilde{Q}_{ii}} = \frac{\frac{\lambda_i}{\sigma_\eta^2}}{1 + \frac{\tilde{Q}_{ii}\lambda_i}{\sigma_\eta^2}} + \gamma = 0. \qquad (3.12)$$

Solving equation (3.12) for $\tilde{Q}_{ii}$ yields

$$\tilde{Q}_{ii} = -\frac{1}{\gamma} - \frac{\sigma_n^2}{\lambda_i} = \alpha - \frac{\sigma_\eta^2}{\lambda_i}, \qquad (3.13)$$

where α is chosen so that $\sum_{i=1}^{N} \tilde{Q}_{ii} = P_T$. It is known that $\tilde{Q}_{ii} \geq 0$, therefore $\tilde{Q}_{ii} = \left(\alpha - \frac{\sigma_\eta^2}{\lambda_i}\right)^+$ where $(\cdot)^+ = \max(0, \cdot)$. Now equation (3.10) becomes

$$\sum_{i=1}^{t}\left(\alpha - \frac{\sigma_\eta^2}{\lambda_i}\right) = P_T, \qquad (3.14)$$

where $t \leq N$ is the number of antennas used to transmit power. Solving (3.14) in terms of α leads to

$$\alpha = \frac{\sigma_\eta^2}{t}\left(\frac{P_T}{\sigma_\eta^2} + \sum_{i=1}^{t}\frac{1}{\lambda_i}\right). \qquad (3.15)$$

Now that α and $\tilde{Q}_{ii}$ are known we can substitute these results into (3.9) to finally obtain

$$C_u = \sum_{i=1}^{t} \log\left(\frac{\lambda_i}{t}\left(\frac{P_T}{\sigma_\eta^2} + \sum_{j=1}^{t}\frac{1}{\lambda_j}\right)\right). \qquad (3.16)$$

3.3 Upper Bound Links Correlation and Capacity

The upper bound (3.5) is important because it provides a direct connection between correlation and capacity. The quality of this newly derived upper bound needs to be examined. In addition, the relationship between capacity and channel correlation needs to be explored.

For purposes of making general observations about the effect of channel correlation, $\mathbf{R}_T$ is assumed to have the form

$$R_{Tij} = r^{|i-j|} \quad \text{where} \quad 0 \leq r \leq 1. \tag{3.17}$$

The quantity $|i - j|$ effectively represents the distance between antennas and r is a measure of the decline in correlation with antenna spacing. By inspection one can see that $r = 0$ yields a completely uncorrelated transmit channel while $r = 1$ models a completely correlated transmit channel. This model is not meant to closely model a specific physical situation but rather to provide insight into the effects of channel correlation on capacity. This model is also useful in assessing the quality of the upper bound (3.5) derived previously.

Let $M = 10$, $N = 10$, and $\frac{P_T}{\sigma_\eta^2} = 30\text{dB}$. Using the correlation model (3.17), the upper bound and ergodic capacity using optimal and uniform power allocation are calculated for different values of r. Figure 3.1 shows the results, using Monte Carlo simulations of (3.2) for the ergodic capacity and (3.5) for the upper bound calculation. For the Monte Carlo simulations, 5000 channel realizations are generated by [28]

$$\mathbf{H} = \mathbf{R}_R^{1/2}\mathbf{G}\mathbf{R}_T^{1/2}, \tag{3.18}$$

where $\mathbf{G}$ is an independent and identically distributed $M \times N$ random matrix whose entries are zero-mean complex-normal distributed and $(\cdot)^{1/2}$ indicates the Cholesky factorization. The matrix $\mathbf{R}_R$ is assumed to be an $M \times M$ identity matrix.
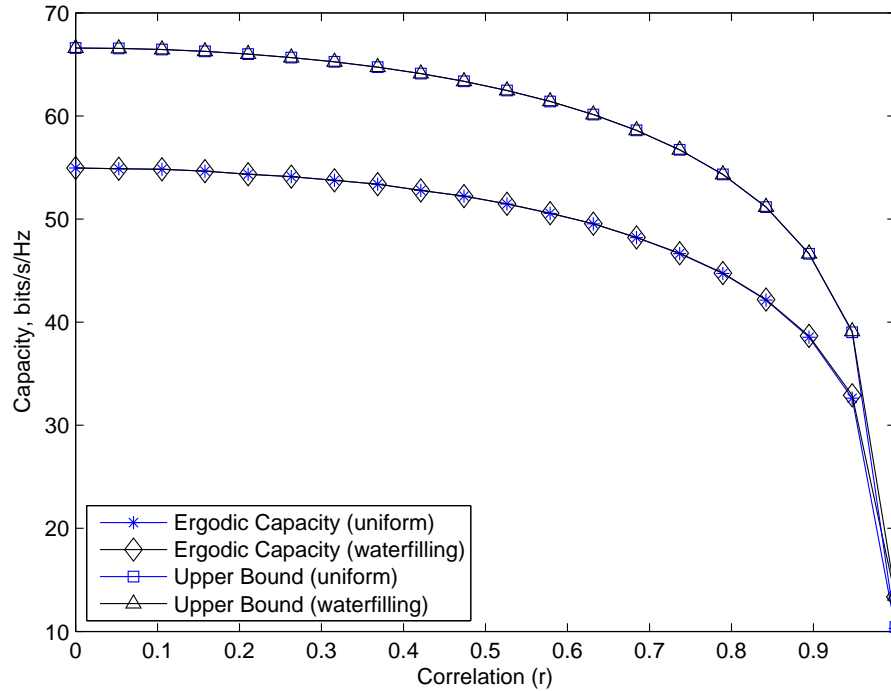
Figure 3.1: Upper bound and ergodic capacity for uniform and optimal power allocation for a $M = 10$, $N = 10$, and SNR = 30dB system.

These results indicate that as the correlation in the channel matrix increases at the transmitter, the capacity of the channel decreases. It also shows that the maximum capacity is obtained when the channel is completely uncorrelated.

It is interesting to note that in Figure 3.1 the water-filling and uniform lines cannot be distinguished because they are so similar. This is expected because in high SNR channels optimal power allocation tends toward uniform allocation. In lower SNR channels the difference in capacity obtained by optimal power allocation and uniform power allocation increases substantially. This can be observed in Figure 3.2 which plots the behavior for an SNR of 15 dB. This result can easily be explained by examining water-filling solution plots for low and high SNR cases. In Figure 3.3 each vertical bar represents a subchannel and the distance between the top of the vertical bar and the water level is representative of the power allocated to that subchannel. These plots clearly illustrate the previous claim that optimal power allocation tends toward uniform power allocation as the SNR increases.

21
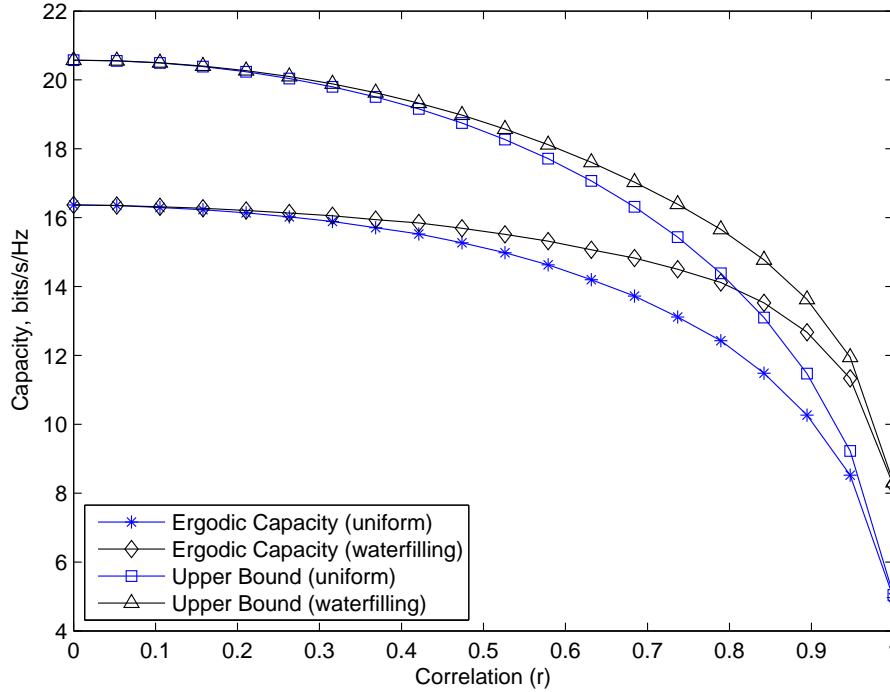
Figure 3.2: Upper bound and ergodic capacity for uniform and optimal power allocation for a $M = 10$, $N = 10$, and SNR = 15dB system.

It is also important to note that the newly derived upper bound (3.16) is a fairly tight bound but also its general behavior with correlation is almost identical to the ergodic capacity. This adds confidence in the quality of the upper bound derived.

3.4 Correlation Reduces Diversity Gain

As explained in Chapter 2, diversity gain of correlated antennas can be computed by creating an equivalent system of uncorrelated antennas with branch gains equal to the eigenvalues of the correlation matrix. This implies that diversity gain is maximized when the channel is uncorrelated [17]. To add confidence to this result and for completeness, the diversity gain of an array of four antennas, relative to a single antenna, is calculated for different channel correlation matrices modeled by (3.17). The results in Figure 3.4 clearly illustrate that diversity gain
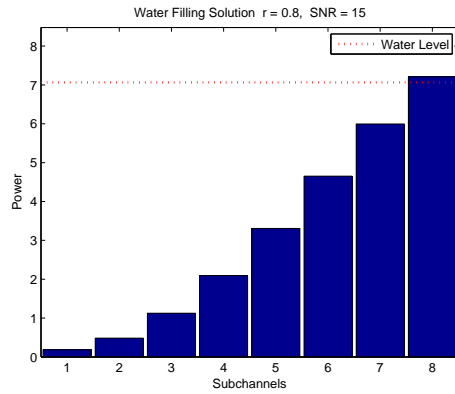
(a) Optimal power allocation for a $M = 10$, $N = 10$, and SNR = 15dB system.
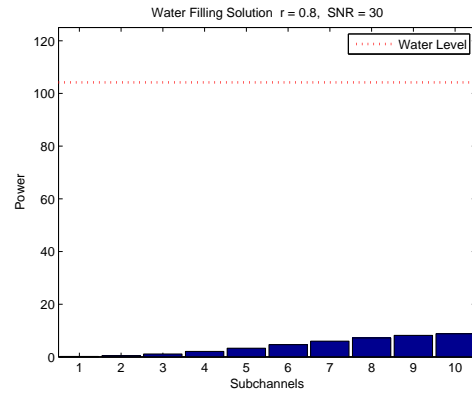
(b) Optimal power allocation for a $M = 10$, $N = 10$, and SNR = 30dB system.

Figure 3.3: (a) At low SNR optimal power allocation is far from uniform. (b) At high SNR optimal power allocation is almost uniform.

is maximized when the channel is uncorrelated and dramatically decreases as the channel becomes highly correlated.
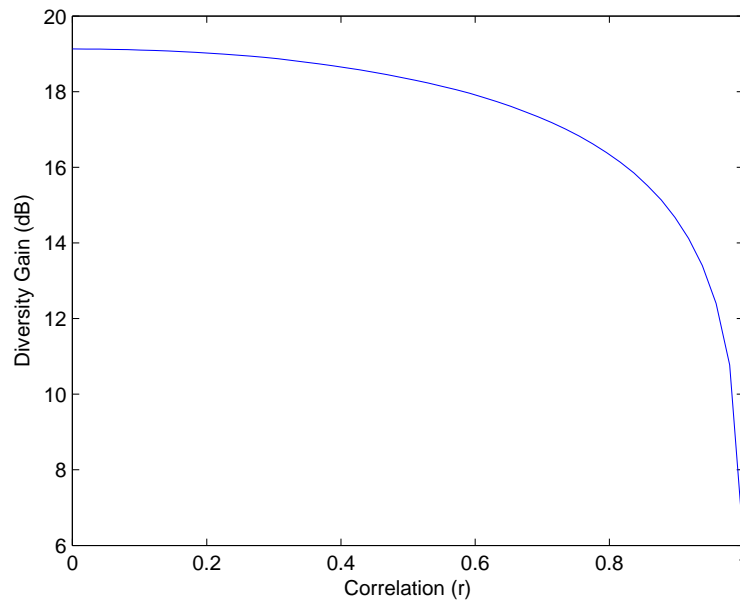
Figure 3.4: Diversity gain of a $M = 4$ and $N = 4$ system vs. channel correlation

3.5 Maximizing Diversity Gain Maximizes Capacity

We have seen that both diversity gain and capacity are highly dependent upon the correlation of the channel. The upper bound derived in Section 3.1 provides an explicit relationship between diversity gain and capacity through the correlation of the channel. Combining the simulation techniques described in Sections 3.3 and 3.4, sample results showing that maximizing diversity gain tends to maximize channel capacity are calculated. Figure 3.5 shows results for a MIMO system with $M = 10$, $N = 10$, and SNR = 20 dB. These results are only meant to illustrate the general relationship between ergodic capacity and diversity gain. Only a general relationship can be demonstrated here because it has only been proven that diversity gain is directly linked to the upper bound of the ergodic capacity but not ergodic capacity itself.
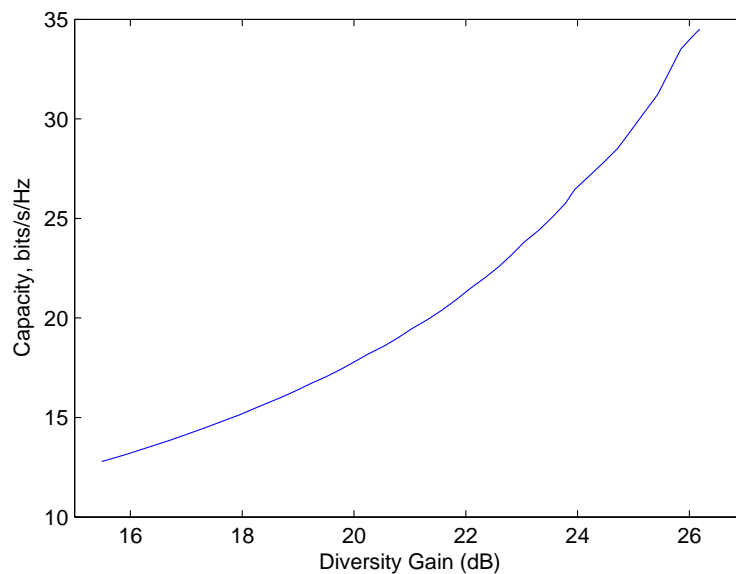
Figure 3.5: Upper bound of ergodic capacity vs. diversity gain for a $M = 10$, $N = 10$, and SNR = 20dB system.

Chapter 4

Near-Optimal Design Methods

As explained in Section 2.5, the research in [9] produces optimal results assuming that overlapping currents can exist. These results, although physically impractical, offer an upper bound for the performance of an array and yield significant insight into practical ways to design an optimal antenna array for a multiple antenna system. This chapter investigates methods for approximating the optimal diversity gain without using overlapping currents.

4.1 Antenna Array Definition

For a design technique to be physically practical, each antenna must be defined as a current distribution over a *unique* aperture. Before optimal or at least near-optimal antenna array elements can be designed, the geometry of the antenna array must be fixed. All of the apertures in the antenna arrays considered in this thesis are squares with the length of their sides being $\lambda/2$. For all of the examples presented in the thesis the $\lambda/2$ by $\lambda/2$ apertures are sampled by a grid of 25 equally spaced pulse functions. Three basic arrangements of these square apertures are examined in this chapter and Chapter 5.

In the first case, four square apertures are arranged to form a larger square which is two apertures by two apertures (λ by λ). The second array consists of four square apertures in a line with a spacing of s between the edges of each element. Unless otherwise stated the spacing, s, is $\lambda/2$. In the third array there are six square apertures equally spaced around a circle of radius r_a. For the examples presented in this thesis the radius of the circle is $r_a = \frac{3}{2}\lambda$. Figure 4.1 shows the three different

array geometries that are examined in this thesis. In this chapter all of the results are for the square array in Figure 4.1(a).
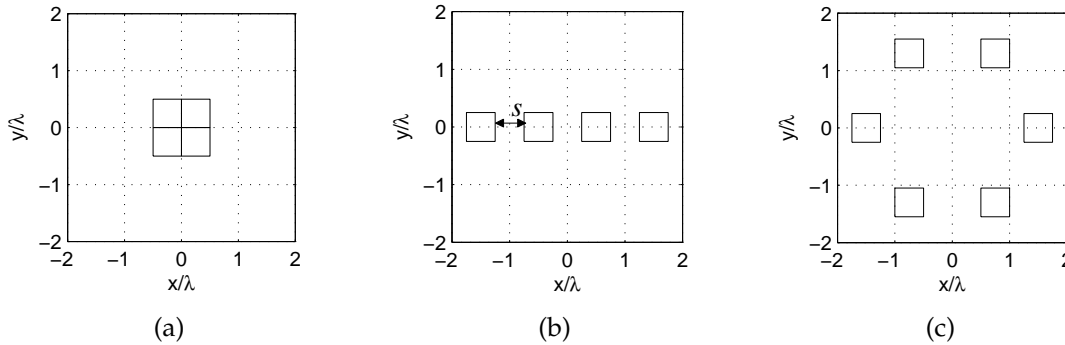
Figure 4.1: (a) Square array. (b) Linear array. (c) Circular array.

4.2 Covariance Approach

Now that some basic antenna array geometries have been defined, approaches can be developed to approximate the optimal overlapping current results. The first approximation approach discussed is perhaps the most straightforward. The fundamental idea behind this approach is that optimizing the performance of each antenna should result in near-optimal performance of the entire array.

To optimize each antenna the optimal design approach described in Section 2.5 is applied to each antenna (aperture) individually. Since overlapping currents are not allowed, only the current distribution associated with the dominant eigenvalue is considered. This method produces the current distributions and antenna patterns shown in Figure 4.3 given the PAS shown in Figure 4.2 and the array geometry in Figure 4.1(a).

It is interesting to note that the antenna patterns and current distributions are identical for each antenna. This is expected because each antenna has the same shape and PAS impinging on it. To gain more insight into the effectiveness of this approach we must refer back to equation (2.11). This approach does a good job of

maximizing the diagonal elements of **R** because each antenna is designed to receive the maximum possible power. However, this approach does not attempt to satisfy the design constraint that the off diagonal elements of **R** should be zero. In fact, since each antenna pattern is the same, the off diagonal elements are actually close to the same magnitude as the diagonal elements for this antenna geometry. Physically this means all of the diversity in this system is coming from the array geometry, not the antenna patterns. This technique can still offer substantial diversity gain improvement over standard dipole arrays, especially when the array elements are well spaced.
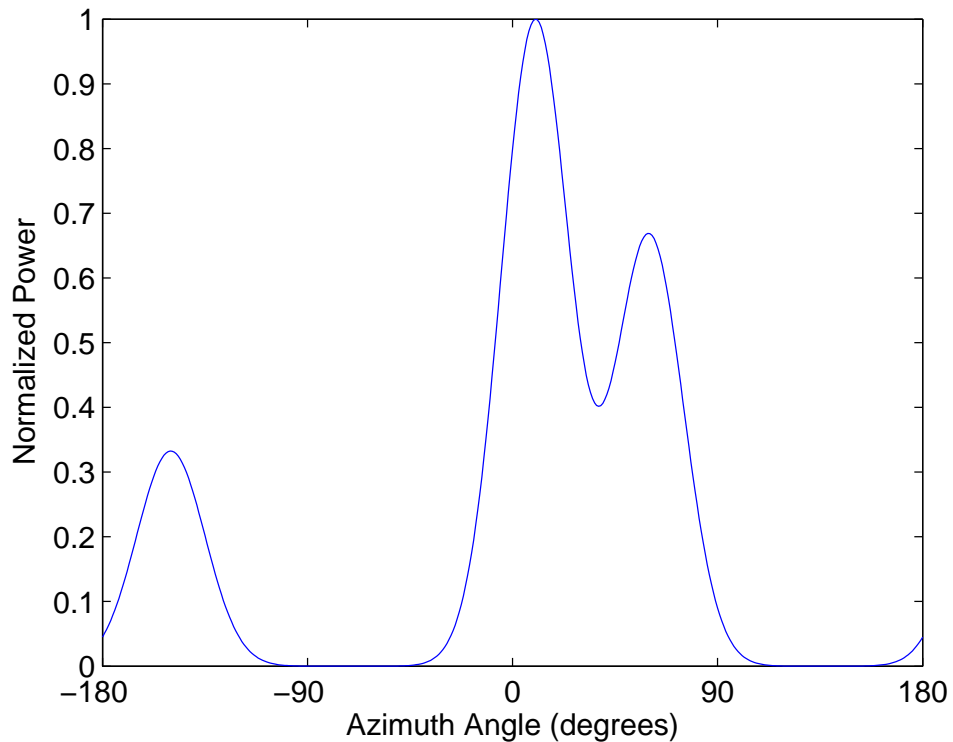
Figure 4.2: Power azimuth spectrum used for the examples in Chapter 4.
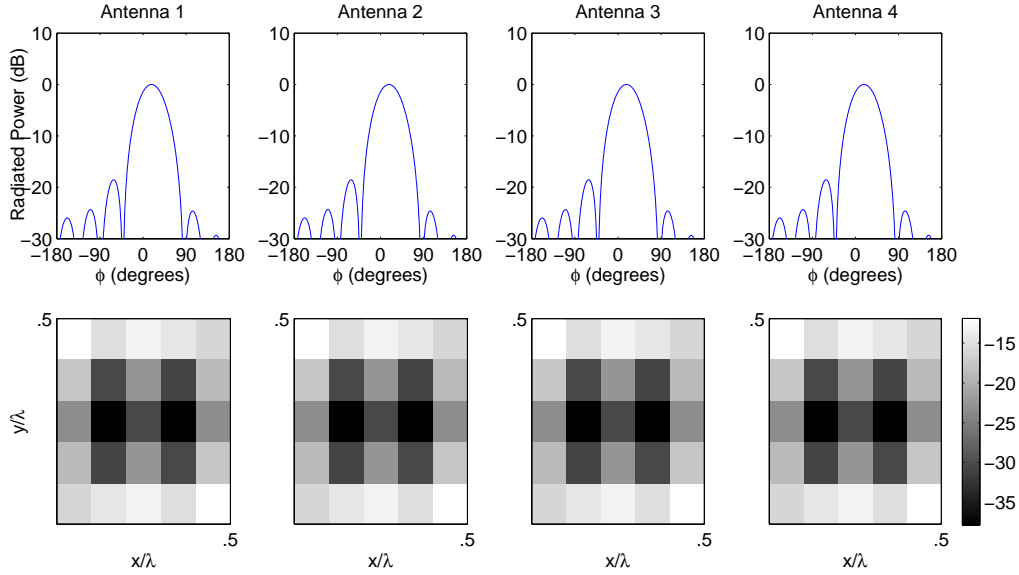
Figure 4.3: Covariance approach approximations of optimal current distributions and antenna patterns.

4.3 Modified Covariance Approach

The covariance approach is appealing because the true optimal design (in terms of power) for each individual antenna can be determined. However, as illustrated previously, the covariance approach does not optimize the *array* for diversity performance. This section discusses a modified covariance approach which attempts to approximate optimal element antenna patterns while minimizing the correlation among antennas.

First, like in the covariance approach, we solve for the optimal current distributions of an individual aperture given a PAS. For the first antenna designed in the array, the current distribution with the largest eigenvalue is selected. So that this method is tractable, the current distributions of the remaining antennas are constrained to be one of the current distributions associated with the four largest eigenvalues. To know which one of these four current distributions should be selected, the diversity gain is calculated with the first antenna's current distribution being fixed and the second antenna's current distribution being each of the possible current distributions. The algorithm then selects the distribution resulting in the

largest diversity gain. Using similar logic, the current distribution for the third antenna is selected to maximize the diversity gain of a three element array. This same procedure is completed for each of the remaining elements of the array.

This design approach is still suboptimal but has a fundamental advantage over the covariance approach. This approach allows diversity to come from the element radiation patterns and the array geometry. It ensures the diagonal elements of **R** are large while attempting to minimize the off diagonal elements of **R**. Note that the average size of the diagonal elements of **R** is smaller using this method than with the covariance method, yet its diversity gain performance is always either equal or superior. Physically this means that power received by each antenna needs to be balanced with the correlation between antennas.

Figure 4.4 shows the current distributions and antenna patterns produced by this method for a square array and the PAS shown in Figure 4.2. In this example the modified covariance approach has a 2.3 dB improvement in diversity gain over that obtained with the covariance approach.
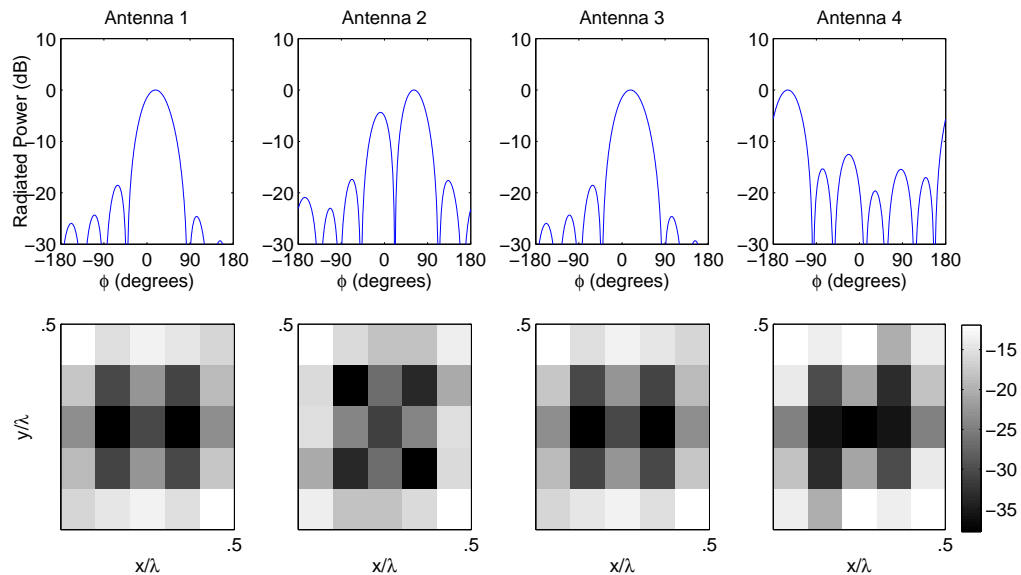
Figure 4.4: Modified covariance approach approximations of optimal current distributions and antenna patterns.

4.4 Current Approach

The current approach attempts to approximate the first D optimal overlapping current distributions for the array with one single current distribution. This is fundamentally different from the previous approach of optimizing each individual antenna independently.

To begin with, the optimal overlapping current approach is performed on the array. Recall that the notation $\mathbf{b}_m$ represents the mth current distribution over the array. Now let $\mathbf{b}_{m,a}$ refer to the mth current distribution over the ath antenna (aperture). For each antenna, a vector $\mathbf{c}_a$ needs to be chosen which approximates the set of vectors $\{\mathbf{b}_{1,a}\ \mathbf{b}_{2,a}\ ...\ \mathbf{b}_{D,a}\}$. To accomplish this a performance metric P_a is defined to be

$$P_a = \max \sum_{i=1}^{D} \Gamma_i \cos^2 \theta_{i,a}, \tag{4.1}$$

where Γ_i is a scalar and $\theta_{i,a}$ is the angle between $\mathbf{b}_{i,a}$ and $\mathbf{c}_a$. By design, this performance metric is maximized when $\mathbf{c}_a$ points in the *average* direction of the $\mathbf{b}_{i,a}$ vectors. Γ_i is chosen to be defined as

$$\Gamma_i = \lambda_i \frac{\left\|\mathbf{b}_{i,a}\right\|^2}{\|\mathbf{b}_i\|^2}, \tag{4.2}$$

where λ_i is the power received by the ith current distribution and $\|\cdot\|$ denotes the 2-norm [26]. The λ_i is included in Γ_i so that dominant current distributions are weighted more heavily. Scaling by $\frac{\|\mathbf{b}_{i,a}\|^2}{\|\mathbf{b}_i\|^2}$ emphasizes basis functions that are important to representing a given optimal current distribution. Using the fact that $\cos \theta_{i,a} = \frac{<\mathbf{b}_{i,a}, \mathbf{c}_a>}{\|\mathbf{b}_{i,a}\|\ \|\mathbf{c}_a\|}$, it can be seen that

$$\cos^2 \theta_{i,a} = \frac{\mathbf{c}_a^{\dagger} \mathbf{b}_{i,a} \mathbf{b}_{i,a}^{\dagger} \mathbf{c}_a}{\left\|\mathbf{b}_{i,a}\right\|^2 \mathbf{c}_a^{\dagger} \mathbf{c}_a}. \tag{4.3}$$

By substituting (4.3) and (4.2) into equation (4.1), P_a becomes

$$P_a = \max \sum_{i=1}^{D} \frac{\lambda_i}{\|\mathbf{b}_i\|^2} \frac{\mathbf{c}_a^\dagger \mathbf{b}_{i,a} \mathbf{b}_{i,a}^\dagger \mathbf{c}_a}{\mathbf{c}_a^\dagger \mathbf{c}_a}. \tag{4.4}$$

P_a needs to be maximized by the choice of $\mathbf{c}_a$. This can be written as

$$\mathbf{c}_a^* = \arg\max_{\mathbf{c}_a} \sum_{i=1}^{D} \frac{\lambda_i}{\|\mathbf{b}_i\|^2} \frac{\mathbf{c}_a^\dagger \mathbf{b}_{i,a} \mathbf{b}_{i,a}^\dagger \mathbf{c}_a}{\mathbf{c}_a^\dagger \mathbf{c}_a}. \tag{4.5}$$

This problem can be solved relatively easily if a few terms are rearranged. Let $\mathbf{B}_a = \sum_{i=1}^{D} \frac{\lambda_i}{\|\mathbf{b}_i\|^2} \mathbf{b}_{i,a} \mathbf{b}_{i,a}^\dagger$. The problem can now be written as

$$\mathbf{c}_a^* = \arg\max_{\mathbf{c}_a} \frac{\mathbf{c}_a^\dagger \mathbf{B}_a \mathbf{c}_a}{\mathbf{c}_a^\dagger \mathbf{c}_a}. \tag{4.6}$$

The vector that maximizes this expression is the eigenvector of $\mathbf{B}_a$ corresponding to the largest eigenvalue of $\mathbf{B}_a$.

This approach is used for each antenna in the array. For the examples presented in this thesis $D = 4$. Figure 4.5 shows the current distributions and antenna patterns produced using this method for a square array and the PAS shown in Figure 4.2.

4.5   Numerical Optimization

The optimal diversity gain, provided that overlapping currents are not allowed to exist, has yet to be calculated. Each of the design approaches presented in this chapter disallows overlapping current but is also suboptimal. To investigate the difference between the theoretical and practical diversity gain limits, numerical optimization is employed. The optimization performed in this section is done using the Nelder-Mead simplex method, with the results from the modified co-variance approach as the initial values. Figure 4.6 shows the current distributions and antenna patterns produced using numeric optimization for a square array and the PAS shown in Figure 4.2. In this situation, disallowing overlapping currents lowered the optimal diversity gain by .59 dB.
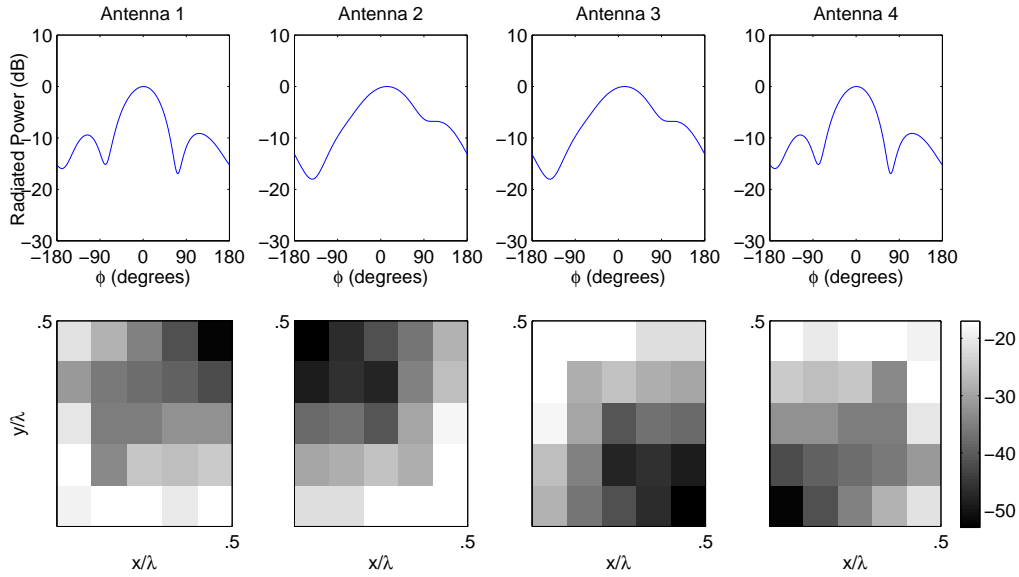
Figure 4.5: Current approach approximations of optimal current distributions and antenna patterns.
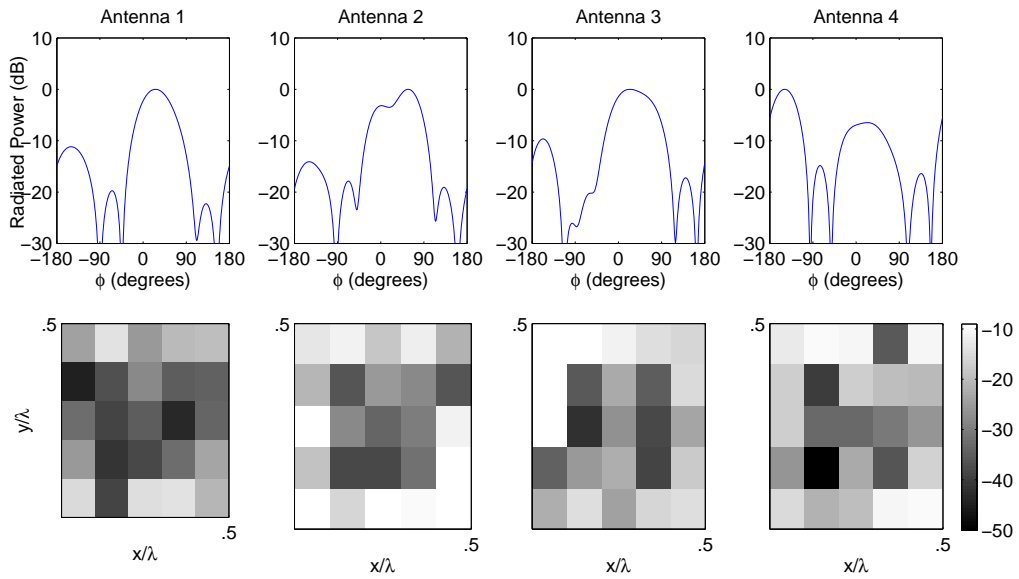
Figure 4.6: Numerically optimized approximations of optimal current distributions and antenna patterns.

The use of this numeric optimization method in this setting is fraught with difficulties. It is extremely computationally intensive compared to the other

methods, especially as the number of basis functions increases. In addition, in this situation, there is no guarantee that the Nelder-Mead simplex method converges to the absolute maximum solution. Surely the efficiency and effectiveness of the numeric methods used here could be improved, but that is not the focus of this work. The purpose of presenting numeric optimization in this thesis is to provide insight into the decreased diversity gain by disallowing overlapping currents.

4.6 Summary of Results

Table 4.1 contains a summary of the diversity gain achieved, in the presence of the PAS shown in Figure 4.2, by each of the design methods explained in this chapter relative to the optimal overlapping current distributions. A more detailed analysis of each design method is presented in Chapter 5.

Table 4.1: Diversity Gain of Each Design Method Relative to the Optimal Overlapping Antennas

Method	Diversity Gain in dB (relative to optimal)
Covariance	-3.7
Modified Covariance	-1.4
Current	-2.3
Numeric Optimal	-0.6

Chapter 5

Analysis of Near-Optimal Design Methods

Now that several different approximation techniques have been presented, each must be analyzed in terms of performance. This chapter attempts to illustrate advantages and disadvantages of the approximation techniques for the array geometries presented in Chapter 4. The effects of array size and multipath characteristics are explored. In addition, the average performance of each design technique and geometry is calculated.

For purposes of comparison and analysis three simple arrays of pulse functions are considered in this chapter. These arrays have the same geometries as the arrays found in Figure 4.1, but have only a single pulse function in the center of each of the apertures. Throughout this chapter, these simple arrays are referred to as dipole arrays because each small pulse function models a Hertzian dipole.

5.1 Effect of Array Size

It is interesting to investigate how the diversity gain produced by each technique varies as a function of the size of the array. To examine this behavior, the diversity gain is calculated using each method on the linear array geometry described in Section 4.1 for values of s between 0 and 3λ, where s is the edge-to-edge spacing of the apertures in the array. For each value of s, the diversity gain of each technique is calculated for an ensemble of 1000 PASs and then averaged to find the mean diversity gain of each technique. Each PAS is randomly generated with 1 to 4 Laplacian clusters. The width of each cluster randomly ranges from 15 to 50 degrees. For this example and throughout this chapter the center angles of the clusters are uniformly distributed over angle and the normalized magnitude of

each is randomly chosen to be between 1 and 10. The PASs are randomly generated this way so that the effects of changing s can be observed over a broad range of PAS shapes. A similar approach is used for analysis throughout the chapter.

The results of this experiment are shown in Figure 5.1. These results show that as the edge-to-edge spacing increases the diversity gain achieved by the modified covariance approach converges to that obtained by the covariance approach. This indicates that once the array size increases beyond a certain value, the element antenna patterns only need to maximize the received power because the antennas in the array receive sufficient diversity from their position alone. Consequently, as the total array aperture size increases, the covariance approach becomes much more useful. It is also interesting to note that the diversity gain of the dipole array and that of the optimal array remain constant after the aperture spacing is larger than one wavelength. This result is intuitive because it implies that diversity gain cannot be increased by an arbitrary amount simply by making the array arbitrarily large for PAS clusters which have a non-zero angle spread. It is surprising how similar the results are for the current and covariance approaches. This is interesting because the two approximation techniques are fundamentally different, yet in this case they yield very similar results.

5.2 Effect of Multipath Characteristics

It would be beneficial to know how the performance of each technique is impacted by basic characteristics of the impinging PAS, such as the number of clusters or the average angular spread of each cluster. In this section the data presented is for an antenna array with the circular geometry as explained in Section 4.1 and shown in Figure 4.1(c). In order to explore trends in performance based on PAS characteristics, two ways of generating the random PAS shapes are considered.

The first investigation focuses on the effect of the number of clusters in the PAS. For this analysis, each PAS is generated using the technique described in Section 5.1, with the exception that the number of clusters is specified deterministically rather than randomly. Figure 5.2 shows the average diversity gain achieved using
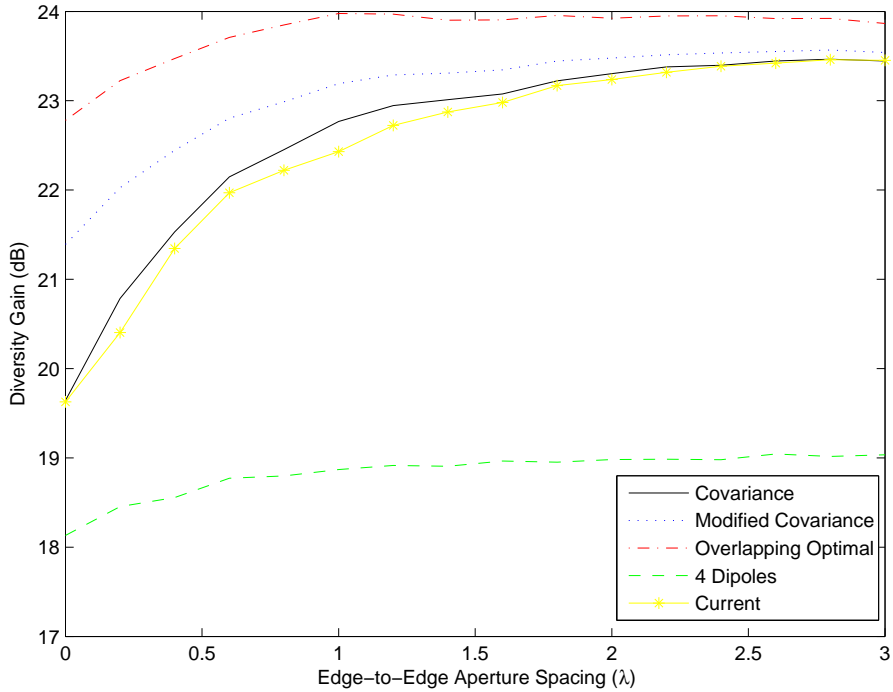
Figure 5.1: Average diversity gain of each approximation technique as a function of the edge-to-edge spacing of apertures in a four element linear array.

each technique as a function of the number of peaks in the PAS, with the average taken over 1000 PAS realizations. These results clearly show that as the number of clusters increases, the diversity gain achieved by the approximate techniques decreases while the diversity gain achieved by a simple dipole array gradually increases. This result is intuitive, since an increase in the number of clusters effectively makes the PAS more uniform over angle. For such a uniform shape, the gain enabled by the subapertures (as compared to the dipole) becomes less beneficial.

The second investigation focuses on the impact of the cluster angular spread on the achievable diversity gain. In this example each PAS has four Gaussian clusters of a set angular spread. Using a process similar to that in the previous examples, for each fixed width of the clusters the diversity gain results are created by averaging the results from 1000 PAS realizations. Figure 5.3 shows the results which are generally similar to those from Figure 5.2. Again, it is seen that as the
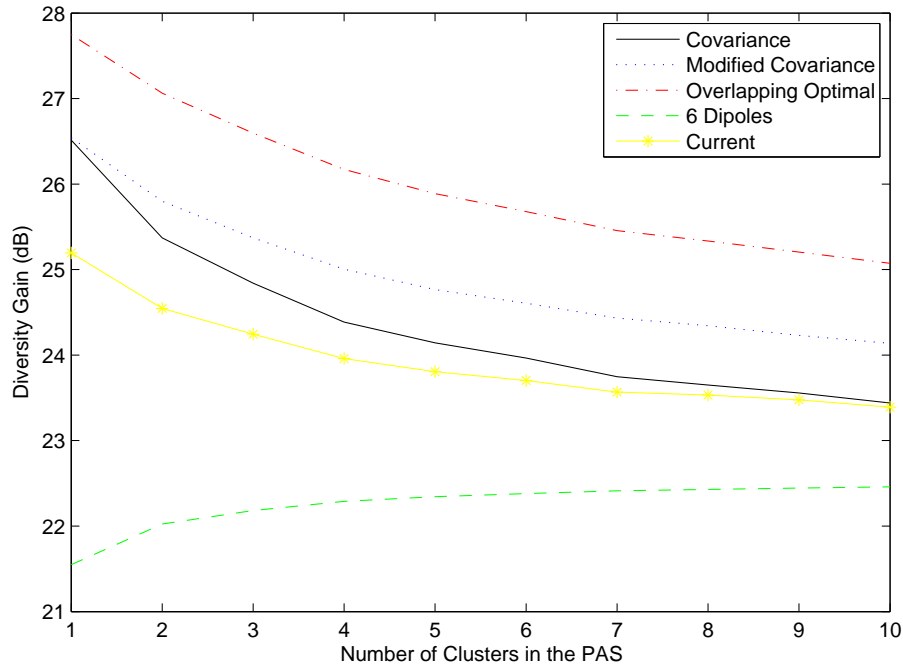
Figure 5.2: Average diversity gain of each approximation technique as a function of the number of clusters in the PAS.

impinging PAS tends to be constant over angle, the performance obtained from all of the approximate techniques begins to converge to that obtained with the simple dipole array. The results also show that the performance of all approximate techniques suffers for narrow clusters, since the antennas are unable to provide narrow beams achieving high gains coupled with the fact that the spatial richness of the multipath decreases. The optimal antennas do not suffer this degradation since each antenna current spans the entire aperture and can therefore offer increased gain which compensates for the reduction in multipath and therefore achievable diversity.

5.3   Comparison of Array Geometries

It is clear from the previous examples that the modified covariance approach has the best average performance, but the question of which array geometry has
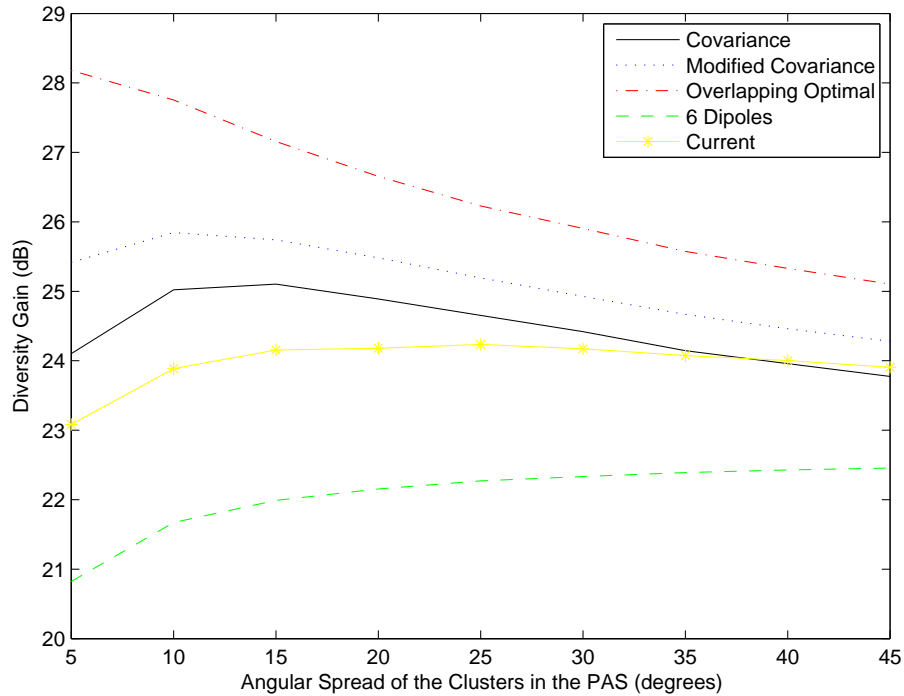
Figure 5.3: Average diversity gain of each approximation technique as a function of the angular spread of clusters in the PAS.

the best performance remains. It is therefore interesting to explore which geometry is best suited for a rich or sparse multipath environment.

In this experiment, instead of calculating the diversity gain relative to a single Hertzian dipole, the diversity gain is calculated relative to a dipole array with the same geometry. This effectively normalizes the diversity gains so that meaningful comparisons can be made between array geometries with varying numbers of elements. To simplify the comparison of the three geometries, only the diversity gains produced using the modified covariance approach are considered.

To test the performance of each array geometry in different multipath environments the experiment described in Section 5.2 is again performed. Figures 5.4 and 5.5 show how the diversity gain achieved by each array changes as the number of clusters increases and the angular spread of each cluster increases, respectively.

The results indicate that these two variations in the PAS have almost an identical impact on the performance for each array.
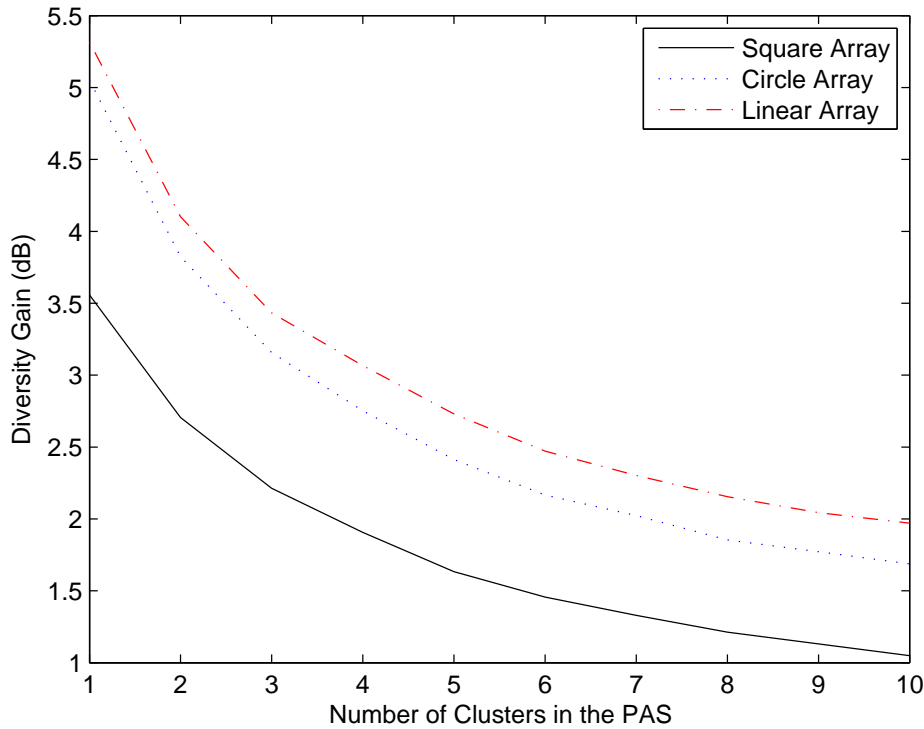
Figure 5.4: Average diversity gain of the modified covariance approach for each geometry as a function of the number of clusters in the PAS.

The average diversity gain performance of each array geometry is calculated by averaging the diversity gain achieved by each geometry for 5000 randomly generated PAS realizations, with the realizations being generated using the approach outlined in Section 5.1. Table 5.1 contains the results of these computations. The results indicate that of the array topologies considered, the linear array is best able to provide diversity gain over a large ensemble of environments. However, it should be emphasized that these results are dependent on the geometries of the apertures used to make up the array. The interdependence of the array and
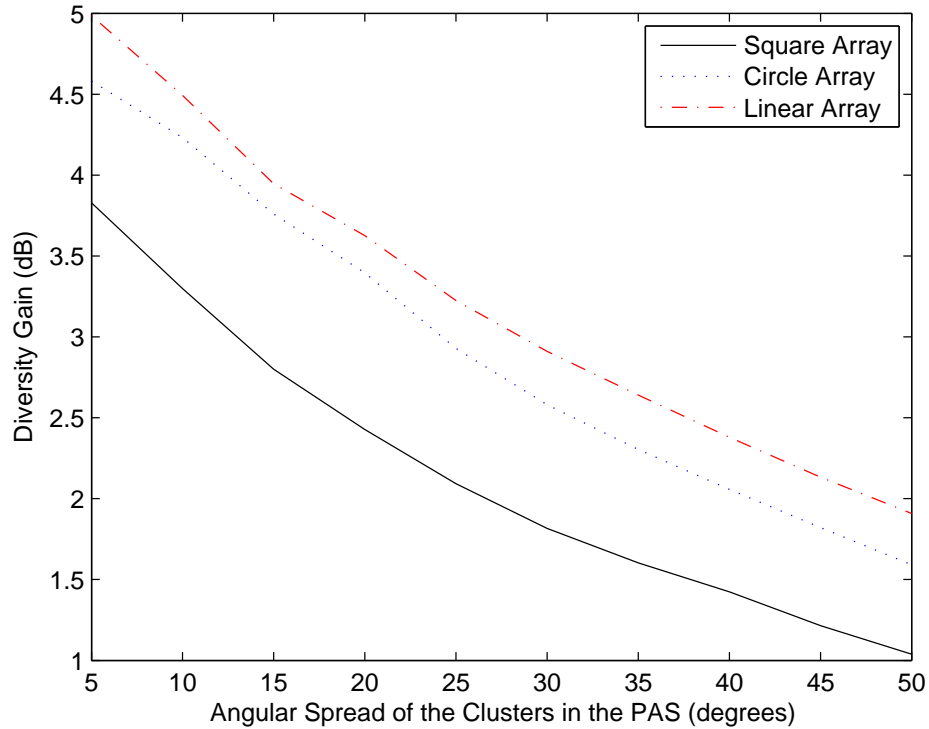
Figure 5.5: Average diversity gain of the modified covariance approach for each geometry as a function of the angular spread of clusters in the PAS.

aperture geometries makes it impossible to say, without further analysis, that a linear array is always best for diversity applications.

Table 5.1: Diversity Gain Using the Modified Covariance Approach For Different Array Geometries

Array Geometry	Square	Circle	Linear
Diversity Gain in dB (relative to array of dipoles)	2.61	3.70	3.98

5.4 Overall Comparisons

A number of examples have been presented in this chapter to investigate the influence of array size or key multipath characteristics on diversity performance.

This section concludes the analysis by presenting average results for each method and array type in the presence of random PASs.

The PASs considered consist of 1 to 7 Laplacian, Gaussian, or Uniform clusters, with the width of each cluster being randomly chosen to lie between 15 and 50 degrees. Table 5.2 summarizes the average results. Each of the design techniques in the table was performed for 5000 PAS realizations except the numeric optimization technique which was performed on 500 realizations due to its intense computational requirements. It is shown that on average the numeric optimization technique achieves a diversity gain about .8 dB below the diversity gain upper bound given by the overlapping current distributions. The results indicate that for the array geometries considered, the modified covariance approach has the best diversity gain performance given this ensemble of multipath environments. Over this ensemble, the diversity gain performance of the modified covariance approach is 1.4 dB below that of the overlapping currents and 3.3 dB higher than that of the simple Hertzian dipole arrays. The circular array offers the highest diversity gain, which is expected because it has six antennas as opposed to four. However, the performance of each of the approximate design methods is most near optimal for the linear array topology.

Table 5.2: Average Diversity Gain of Each Design Technique and Array Geometry

Array Type	Square	Linear	Circular
Overlapping Optimal	22.1	23.5	26.6
Numeric Optimal	21.4	22.6	25.7
Dipoles	18.0	18.4	21.8
Covariance	18.5	21.6	24.5
Modified Covariance	20.7	22.3	25.3
Current	19.5	21.5	24.2

Chapter 6

Conclusion

A key contribution of this work is the derivation and verification of an ergodic capacity upper bound that directly links good diversity performance to good ergodic capacity. This bound is verified by simulation and used to prove that maximizing diversity gain is a valid technique to achieve good ergodic capacity. Among other things, proving this direct correlation between diversity and ergodic capacity adds validity to the design goal of maximizing diversity gain and reinforces the importance of the work presented in [9].

The optimal design approach derived in [9] is reviewed here. This approach is the basis of most of the work presented in this thesis. Although the solutions to this optimal design approach are impossible to implement, they provide both an upper bound for diversity performance and a starting point for practical closed form design methods.

Another contribution of this thesis is the development of several different design approaches to approximate the optimal non-overlapping current distributions in the presence of a known PAS. Although each one of the developed design methods is a suboptimal approximation, some of the methods achieve near-optimal diversity performance. Multiple approximation techniques are presented because each approximation method is fundamentally different.

This thesis clearly explains how each design technique attempts to maximize diversity gain and develops insight into the effectiveness of each approach. The covariance approach attempts to maximize diversity gain by maximizing the power received by each antenna. For this approach to work well the array geometry must create significant diversity because no diversity is introduced through the

antenna patterns. An approach which is a modification to the covariance approach balances maximizing the power received by each antenna with minimizing the cross-correlation of the antennas to maximize diversity gain. Significant gains are achieved by this approach over the covariance approach when the antenna elements are closely packed. The current approach attempts to create a current distribution that effectively spans the space defined by the four dominant optimal current distributions. This approach is particularly ill-suited to form narrow beams, but its performance is similar to that of the covariance approach on average.

The optimal design approach from [9] is used as a theoretical upper bound in this thesis. This thesis contributes to this bound by showing that currents restricted to be non-overlapping can come on average to within 0.8 dB of the theoretical optimal diversity gain, although numeric optimization is used to achieve this performance.

The performance of three different array geometries is investigated. From the analysis performed, each geometry appears to react very similarly to variations in the richness of the multipath. Overall, the circular array offers the highest diversity gain because it contains two more antennas than the other arrays. In a more meaningful comparison, the linear aperture array is shown to be the array that outperforms its corresponding dipole array by the most.

A noteworthy contribution of this thesis is that in very rich multipath environments an array of dipoles can produce diversity gains within 2 dB of the diversity gains achieved by much more complicated arrays of the same geometry. In typical multipath environments arrays designed with the modified covariance approach outperform dipole arrays by about 3 dB. In sparse multipath environments the improvement is even greater, averaging about 5 dB. These figures could be very useful to someone deciding whether it is worth investing time and effort to create an array with near-optimal diversity gain.

In addition to what is presented in this thesis, significant future work could be completed. Work could be done to improve the numeric optimization technique implemented both to improve efficiency and to guarantee that the optimizer will

converge to an absolute maximum. If this numeric optimization technique were developed it could become a practical design approach, especially for situations where the PAS is constant. In this thesis all of the antennas have a $\lambda/2$ by $\lambda/2$ aperture, but future research could be focused on the diversity performance of each design approach as a function of aperture size and shape. Further research could also be conducted to explore the interdependence of the aperture and array geometries. Using this information, the array and aperture geometries that yield the best diversity when combined could be determined.

Bibliography

[1] G. Foschini and M. Gans, "On limits of wireless communications in a fading environment when using multiple antennas," *Wireless Personal Communications*, vol. 6, no. 1, pp. 311–335, 1998.

[2] C. Martin, J. Winters, and N. Sollenberger, "MIMO radio channel measurements: Performance comparison of antenna configurations," *Vehicular Technology Conference*, vol. 2, pp. 1225–1229, 2001.

[3] J. Wallace and M. Jensen, "Intrinsic capacity of the MIMO wireless channel," *Vehicular Technology Conference*, vol. 2, pp. 701–705, 2002.

[4] M. Jensen and J. Wallace, "A review of antennas and propagation for MIMO wireless communications," *IEEE Transactions on Antennas and Propagation*, vol. 52, no. 11, pp. 2810–2824, November 2004.

[5] C. Waldschmidt, T. Fugen, and W. Wiesbeck, "Spiral and dipole antennas for indoor MIMO-systems," *IEEE Antennas Wireless Propagation Letters*, vol. 1, no. 1, pp. 176–178, 2002.

[6] T. Svantesson, "Correlation and channel capacity of MIMO systems employing multimode antennas," *IEEE Transactions Veh. Technol.*, vol. 51, pp. 1304–1312, Nov. 2002.

[7] D. A. Gore, R. W. Heath, and A. Paulraj, "Transmit selection in spatial multiplexing systems," *IEEE Communication Letter*, vol. 6, pp. 491–493, Nov. 2002.

[8] A. F. Molisch, J. H. Winter, and M. Z. Win, "Capacity of MIMO systems with antenna selection," in *Proc. IEEE Int. Conf. Communications*, vol. 2, Helsinki, Finland, June 11-14, 2001, pp. 570–574.

[9] B. T. Quist, "Synthesis of optimal arrays for MIMO and diversity systems," Master's thesis, Brigham Young University, Provo, Utah, December 2007.

[10] E. Biglieri, R. Calderbank, A. Constantinides, *et al.*, *MIMO Wireless Communications*. Cambridge University Press, 2007.

[11] I. Telatar, "Capacity of multi-antenna Gaussian channels," *European Transactions on Telecommunications*, vol. 10, no. 6, pp. 585–595, 1999.

[12] D. W. Bliss, K. W. Forsythe, A. O. Hero, and A. L. Swindlehurst, "MIMO environmental capacity sensitivity," *IEEE Proc. 34th Asilomar Conf. Signals, Systems, Computers*, pp. 764–768, 2000.

[13] S. A. Jafar, S. Vishwanath, and A. Goldsmith., "Channel capacity and beamforming for multiple transmit and receive antennas with covariance feed back," *ICC*, vol. 7, pp. 2266–2270, June 2001.

[14] S. A. Jafar and A. Goldsmith, "Multiple-antenna capacity in correlated Rayleigh fading with channel covariance information," *IEEE Transactions on Wireless Communications*, vol. 4, no. 3, pp. 990–997, May 2005.

[15] N. Skentos, A. Kanatas, P. Dallas, and P. Constantinou, "MIMO channel characterization for short range fixed wireless propagation environments," *Wireless Personal Communications*, vol. 36, no. 4, pp. 339–361, March 2006.

[16] D. G. Brennan, "Linear diversity combining techniques," *Proc. IRE*, vol. 47, no. 6, pp. 1075–1102, Jun. 1959.

[17] O. Nørklit, P. D. Teal, and R. G. Vaughan, "Measurement and evaluation of multi-antenna handsets in indoor mobile communication," *IEEE Trans. Antenna and Propagation*, vol. 49, no. 3, pp. 429–437, 2001.

[18] L. Schumacher, K. Pedersen, and P. Mogensen, "From antenna spacings to theoretical capacities - guidelines for simulating MIMO systems," *Proc. 2002 IEEE 13th Intl. Symp. on Personal, Indoor and Mobile Radio Comm.*, vol. 2, pp. 587–592, 2002.

[19] K. Pedersen, P. Mogensen, and B. Fleury, "A stochastic model of the temporal and azimuthal dispersion seen at the base station in outdoor propagation environments," *IEEE Transactions on Vehicular Technology*, vol. 49, no. 2, pp. 437–447, March 2000.

[20] L. Dong, H. Choo, H. R. W. Jr., and H. Ling, "Simulation of MIMO channel capacity with antenna polarization diversity," *IEEE Transactions on Wireless Communications*, vol. 4, no. 4, pp. 1869–1873, July 2005.

[21] J. A. Kong, *Electromagnetic Wave Theory*. John Wiley and Sons, 1990.

[22] N. Bikhazi and M. Jensen, "The relationship between antenna loss and superdirectivity in MIMO systems," *IEEE Trans. Wireless Communications*, vol. 6, no. 5, pp. 1796–1802, May 2007.

[23] A. Goldsmith, S. A. Jafar, N. Jindal, and S. Vishwanath, "Capacity limits of MIMO channels," *IEEE Journal on Selected Areas in Communications*, vol. 21, no. 5, pp. 684–702, 2003.

[24] T. Cover and J. Thomas, *Elements of Information Theory*. New York: Wiley, 1991.

[25] S. K. Jayaweera and H. V. Poor, "On the capacity of multi-antenna systems in the presence of Rician fading," in *Vehicular Technology Conference*, vol. 4, Fall 2002, pp. 1963–1967.

[26] T. K. Moon and W. C. Stirling, *Mathematical Methods and Algorithms for Signal Processing*. Upper Saddle River, NJ: Prentice Hall, 2000.

[27] S. Loyka and A. Kouki, "New compound upper bound on MIMO channel capacity," *IEEE Communications Letters*, vol. 6, no. 3, pp. 96–98, March 2002.

[28] K. Yu, M. Bengtsson, B. Ottersten, D. McNamara, *et al.*, "Modeling of wideband MIMO radio channels based on nlos indoor measurements," *IEEE Transactions on Vehicular Technology*, vol. 53, no. 3, pp. 655–665, May 2004.